Semi-flexible polymers at a liquid–liquid interface: Self-consistent field calculations

Marcel C. P. van Eijk and Frans A. M. Leermakers

Citation: J. Chem. Phys. **109**, 4592 (1998); doi: 10.1063/1.477064
View online: http://dx.doi.org/10.1063/1.477064
View Table of Contents: http://jcp.aip.org/resource/1/JCPSA6/v109/i11
Published by the American Institute of Physics.

Semi-flexible polymers at a liquid–liquid interface: Self-consistent field calculations

Marcel C. P. van Eijk[a] and Frans A. M. Leermakers
Wageningen Agricultural University, Laboratory for Physical Chemistry and Colloid Science, Dreijenplein 6, 6703 HB Wageningen, The Netherlands

(Received 13 January 1998; accepted 11 June 1998)

The adsorption of semi-flexible polymers at a liquid–liquid interface largely differs from that at a solid surface. The width of the interface is an additional length scale in the problem, making the system behavior particularly rich. We consider two phase-separating monomeric liquids, C and D, and a polymer A_N which dissolves equally well in both liquids. We study this system in a self-consistent field model in the dilute regime. The stiffness of the polymer is controlled by the use of a rotational isomeric state approach. We show that the interfacial width ξ, the persistence length q, and the chain length N are relevant parameters in the adsorption behavior. A key observation is that, while keeping $N^{1/2}/\xi$ constant, the adsorbed amount goes through a minimum with increasing q/ξ. An initial increase of q/ξ ($q/\xi \lesssim 1$) effectively leads to a larger coil size, leading to a decrease of the adsorbed amount. However, when $q/\xi \gg 1$, alignment of parts of the polymer within the interfacial region occurs due to the lack of entropic penalties. This alignment process induces an increase of the adsorbed amount. These observations also have implications for the ongoing discussion, which species shows preferential adsorption in a mixture of flexible and stiff polymers. In this discussion one should consider the effects of the finite size of the interfacial region. © *1998 American Institute of Physics.* [S0021-9606(98)50835-5]

I. INTRODUCTION

The adsorption of macromolecules at liquid–liquid interfaces is of major importance in a wide variety of relevant systems, ranging from food products to oil recovery. The flexibility of a polymer should have an effect on its adsorption behavior, but an *a priori* statement about the precise nature of these effects cannot be given from simple considerations. Most theoretical adsorption studies on semi-flexible polymers consider a solid surface, where the problems associated with the boundary condition usually do not receive much attention. Monte Carlo simulations on a mixture of flexible and stiff short chains show that the stiff chains near a Fresnel interface (i.e., infinitely sharp) are the most surface active.[1,2] On the other hand, using an analytical self-consistent field (SCF) theory, Wu *et al.*[3] report the opposite. The apparent conflict in these results probably has its origin in the choice of the definition of the solid surface. In the former an infinitely sharp interface is used, whereas in the latter case a fairly sharp but smooth density profile is assumed. Both choices for the interface are bound by the numerical schemes applied in the different SCF theories. The chosen schemes imply certain boundary conditions which cannot be circumvented. In other words the chosen scheme determines which systems are accessible and which are not.

In the present paper we like to take an alternative route to by-pass the problems associated with a solid–liquid interface. By using a liquid–liquid interface, we not only circumvent the problem of an *ad hoc* choice of the boundary condition, but are also able to control the width of the interfacial region. We will use a numerical SCF theory to study the behavior of a polymer A_N near an interface formed by the phase boundary of two monomeric liquids. By varying the Flory-Huggins interaction parameter between the two solvents, we are able to control the interfacial width. We apply a rotational isomeric state (RIS) model to vary the stiffness of the polymer chain, and study its influence on the adsorption behavior. Other parameters in our calculations are chosen such that the analysis of the adsorption process is relatively easy. We will show that the interfacial width (to be defined below) is a relevant parameter, even when this width is small. In particular we will concentrate on the interplay between this parameter and the persistence length of the polymer. Obviously, the length of the polymer and the solvent strength (effective adsorption energy) are additional parameters in the system.

II. THEORY

A. General formulation of the model

We consider a lattice model of a 3-component system, containing two monomeric components, denoted by C and D, and one polymer A_N, where N denotes the number of constituting units. We choose the interaction parameters such that the two monomeric components phase separate, creating a liquid–liquid interface at which polymer adsorption can occur. We examine the system not too far from its critical point, using the interfacial width as a tuning parameter. However, we have to keep in mind that this width must be substantially smaller than the system size to avoid boundary

[a]Current address: Aalborg University, Biotechnology Laboratory, Sohngårdsholmsvej 57, 9000 Aalborg, Denmark.
E-mail: i5mars@civil.auc.dk

effects. In line with this, we will keep the overall polymer concentration low in order to minimize the effect of added polymer on the interfacial width and on the location of the Gibbs dividing plane. Adsorption from dilute solution will be limited to the Henry regime, i.e., polymer overlap does not play a decisive role. Starting from the lattice model, there are several ways to evaluate the properties of the system. We will discuss two possible approaches: an analytical and a numerical mean-field theory. We will use the analytical approach to describe the system without polymer, and the numerical one to incorporate the polymer.

B. Analytical mean-field approach

As long as the polymer concentration is low, some characteristics of the system can already be deduced from the properties of the binary mixture of the monomeric components. These characteristics can be used to determine which parameters should be varied to access interesting regions of the ternary system. We are interested in the behavior of this system beyond its critical point, i.e., it consists of a *C*-rich and a *D*-rich phase. We consider the system to be described by the exact Hamiltonian $\mathcal{H}$, leading to the probability distribution function

$$P \propto \exp\left(-\frac{\mathcal{H}}{k_B T}\right). \tag{2.1}$$

The total Helmholtz energy (or free energy) of our system, given in terms of P is given by

$$\mathcal{F} = k_B T \int d\Lambda P \ln P + \int d\Lambda P \mathcal{H}, \tag{2.2}$$

where Λ represents the phase space of the system. Minimization of this exact free energy is not possible, but requires a variational approximation to the Boltzmann weight. We consider a model system, described by a Hamiltonian $\mathcal{H}_0$, and minimize Eq. (2.2) with respect to the constituting parameters of the model system. The free energy is now approximated by

$$F = k_B T \int d\Lambda P_0 \ln P_0 + \int d\Lambda P_0 \mathcal{H}, \tag{2.3}$$

where $P_0 \propto \exp(-\mathcal{H}_0/k_B T)$. The exact free energy $\mathcal{F}$ is bound by the inequality[4]

$$\mathcal{F} < F = F_0 + \langle \mathcal{H} - \mathcal{H}_0 \rangle_0. \tag{2.4}$$

Here, F_0 denotes the free energy of the model system and averaging is carried out with respect to $\exp(-\mathcal{H}_0/k_B T)$.

An easy way to access the properties of a binary mixture is the use of an Ising model (see, e.g., Ref. 5). In Appendix A a mean-field approximation of this model is discussed and the relevant equations within this approach are given. For a system not too far from its critical point, the reduced density ρ of component D as a function of the distance z from the interface is given by substitution of the equation into Eq. (A19), which leads to

$$\rho(z) = \frac{1}{2} + \sqrt{\frac{\chi - 2}{24 b^3}} \tanh \frac{z}{\xi}, \tag{2.5}$$

where the interfacial width, or bulk correlation length, is given by

$$\xi = b \sqrt{\frac{2\lambda_1 \chi}{\chi - 2}}. \tag{2.6}$$

In these equations b denotes the nearest-neighbor distance, χ is the Flory-Huggins interaction parameter, and λ_1 accounts for the relative number of nearest neighbors of a segment in the direction of the reduced density gradient.

We will use the interfacial width from Eq. (2.6) as a tuning parameter for the self-consistent field calculations, where polymer is incorporated into the system. In doing this, we take special care that the addition of a small amount of polymer to the system does not change the interfacial width significantly. One should also bear in mind that Eq. (2.6) is only valid rather close to the critical point, i.e., $\chi - 2 \ll 1$.

C. Numerical self-consistent field theory

We used the self-consistent field (SCF) formalism developed by Scheutjens and Fleer (SF),[6,7] which was originally set up to study polymer adsorption from dilute or semi-dilute solution onto solid surfaces. We will only discuss some basic aspects of the theory, and touch upon the assumptions made in it. Finally, we will mention some extensions to this theory, which make it suitable for the liquid–liquid interface system in the presence of semi-flexible polymer.

The SF SCF approach is a mean-field lattice theory, where only one of the three spatial coordinates remains as a variable, whereas in the other directions density gradients are averaged out. One should bear in mind that this theory starts from the same assumptions as the aforementioned mean-field approximation to the Ising model. However, no Taylor expansion of the free energy density is needed. Therefore, the theory is especially valuable away from the critical point, but it can also be used in the neighborhood of the critical point as long as the correlation length does not exceed the system size. In this SCF model a test molecule is situated in a one-dimensional potential field, set up by the other components in the system. All the possible conformations of the test molecule are generated using Markoffian statistics, and these are weighted with the local potential field. Appropriate normalization leads to the composition profile of the system. The potential field is a functional of the reduced density profile and this profile is, in turn, itself a functional of the potential field. The goal of the SF SCF approach is to find a unique solution to this problem, which involves the choice of proper boundary conditions and constraints.

In the SF SCF theory all molecules are built up from equally sized segments and are placed on a lattice. The lattice is composed of m parallel layers of thickness b, where the layers are numbered $i = 1,2,\ldots,m$. The lattice is furthermore characterized by so-called *a priori* step probabilities λ_{ij}, which give the relative number of contacts of a segment in layer i with those in layer j. Obviously, $\lambda_{ij} = 0$ if $|j - i| > 1$, and $\Sigma_{j=1}^{m} \lambda_{ij} = 1$. We will use the notation λ_0 for $i = j$, and λ_1 for $|j - i| = 1$. For the calculation of the composition profile we define the local reduced density (in layer i) for segment type x as $\rho_x(i) = n_x(i)/l$, where $n_x(i)$ denotes the

number of segments of type x in layer i, and l is the number of sites in every layer. We denote molecule related quantities by an index α. The segments constituting molecule α are numbered $s=1,2,\ldots,N_\alpha$. The local reduced density of a segment type can also be expressed in terms of the local reduced density $\rho_\alpha(i,s)$ of segment s of molecule α:

$$\rho_x(i)=\sum_\alpha \sum_{s=1}^{N_\alpha} \rho_\alpha(i,s)\,\delta_\alpha(s,x), \tag{2.7}$$

where $\delta_\alpha(s,x)$ is defined as being unity if segment s of molecule α is of type x and zero otherwise.

We only take into account nearest-neighbor interactions, which are accounted for by the Flory-Huggins interaction parameter χ_{xy} between segments x and y. The imposed mean-field approximation causes the interactions within one layer to be smeared out. The potential energy $u_x(i)$ of a segment in layer i with respect to the bulk (in our case the C-rich phase) is then by

$$u_x(i)=u'(i)+k_BT\sum_y \chi_{xy}(\langle\rho_y(i)\rangle-\rho_y^b), \tag{2.8}$$

where the angular brackets indicate the weighted average over layers $i-1$, i, and $i+1$, which is needed to account for the nearest-neighbor interactions. The first term in Eq. (2.8), u', is a Lagrange field to ensure that the total reduced density is constant, i.e.,

$$\sum_x \rho_x(i)=1 \quad \forall i. \tag{2.9}$$

Next, we define the segment weighting factor $G_x(i)=\exp(-u_x(i)/k_BT)$, which is just a Boltzmann factor of the field for segment x. In order to account for chain connectivity the end-segment weighting factors $G_\alpha(i,s|1)$ and $G_\alpha(i,s|N_\alpha)$ are introduced, defined as the average statistical weight of all conformations with segment s in layer i and the first or last segment, respectively, located anywhere in the system. They can be calculated by a propagator scheme

$$G_\alpha(i,s|1)=G_\alpha(i,s)\langle G_\alpha(i,s-1|1)\rangle, \tag{2.10a}$$

$$G_\alpha(i,s|N_\alpha)=G_\alpha(i,s)\langle G_\alpha(i,s+1|N_\alpha)\rangle, \tag{2.10b}$$

where the angular brackets again indicate the weighted average over layers $i-1$, i, and $i+1$. This averaging assures the chain connectivity.

In the original SF SCF approach a first-order Markoffian approximation is used, which is characterized by the so-called connectivity law

$$\rho_\alpha(i,s)=C_\alpha\frac{G_\alpha(i,s|1)G_\alpha(i,s|N_\alpha)}{G_\alpha(i,s)}, \tag{2.11}$$

where C_α is a normalization constant which, in an open system, is most conveniently written as $C_\alpha=\rho_\alpha^b/N_\alpha$. The free segment weighting factor for segment s in molecule α is given by $G_\alpha(i,s)=\Sigma_x G_x(i)\,\delta_x(i,s)$. It is needed in the numerator of Eq. (2.11) to correct for double counting of the statistical weight of segment s.

The fundamental equations of the SF SCF approach, given above, set the stage for our system. The presence of a liquid–liquid interface implies the following boundary conditions

$$\rho_x(0)=\rho_x(1), \quad \rho_x(m+1)=\rho_x(m), \tag{2.12}$$

i.e., the system has reflecting boundaries on either side. One of the features which is not described by the presented equations is the chain stiffness. Introduction of this property involves a change in the connectivity law from Eq. (2.11) and requires another propagator scheme [Eq. (2.10)]. In modeling association colloids, Leermakers *et al.* implemented a rotational isomeric state (RIS) approach in the SCF theory to include chain stiffness.[8] In this way local self-avoidance of the chains is accounted for, and chain rigidity can be controlled by changing the energy difference Δu_{tg} between the *trans* and the *gauche* states. Because no fundamental change in the theory occurs, we will not give a full description of the implementation here but refer to the literature.[8] Basically, the RIS approach implies the use of third-order Markoffian statistics in the SCF theory. The exact consequences of this approach to the chain stiffness will be discussed in the next section.

Our system consists of $m=300$ lattice layers and the number of sites per layer is conveniently chosen as $l=1$. In planar systems, however, this latter choice is irrelevant, because all quantities are calculated using densities and energies per site. Because of the RIS model, it is convenient to use a tetrahedral lattice, which ensures that the connectivity constraints are based on the same lattice as the nearest-neighbor interactions.[8] The tetrahedral lattice is characterized by $\lambda_1=1/4$. The monomeric component C is used as solvent and the total amount of D in the system is $\Theta_D=150$. The bulk concentration of polymer A_N is chosen to be $\rho_A^b=10^{-5}$, which, in our case, is in the dilute regime. The interaction parameters of the A-segments with both liquids are $\chi_{AC}=\chi_{AD}=0$ throughout the paper. This choice makes the system symmetric for the polymer. A correct choice of χ_{CD}, simply denoted as χ, ensures a phase separation, and thus the presence of an interface. The critical point of phase separation $(\rho_{A,c},\chi_c)$ is found by solving

$$\left(\frac{\partial^2 f}{\partial\rho_C^2}\right)_{\rho_{C,c}}=0, \tag{2.13}$$

where f is the Helmholtz free energy per site for a homogeneous system, which in the random mixing approximation is for the ternary system given by [see Eq. (A11)]

$$\frac{f}{k_BT}=\rho_C\ln\rho_C+(1-\rho_C-\rho_A)\ln(1-\rho_C-\rho_A)+\frac{\rho_A}{N}\ln\rho_A+\chi\rho_C(1-\rho_C-\rho_A). \tag{2.14}$$

At the critical point $\rho_{C,c}=\rho_{D,c}$, so the solution of Eq. (2.13) is

$$\chi_c=\frac{2}{1-\rho_A}, \quad \rho_{C,c}=\frac{1-\rho_A}{2}. \tag{2.15}$$

Because the polymer concentration is low, the total amount of C is given by $\Theta_C = 150 - \mathcal{O}(m\rho_C^b)$. The exact value of Θ_C is such that the Gibbs dividing plane is located on the boundary of layers 150 and 151, which prevents lattice artifacts from playing a role. We define the distance from the interface as $z = (i - 150.5)b$.

D. Chain dimensions

The adsorption of a polymer at a liquid–liquid interface will depend on the dimensions of the polymer. Within a homopolymer at least two different length scales can be distinguished. We will consider the end-to-end distance $\langle R^2 \rangle^{1/2}$ and the persistence length q as the relevant length scales. These quantities are defined in terms of the bond vectors $\mathbf{r}_i$ and the number of bonds L as follows

$$\langle R^2 \rangle \equiv \sum_{i=1}^{L} \sum_{j=1}^{L} \langle \mathbf{r}_i \cdot \mathbf{r}_j \rangle, \tag{2.16}$$

$$q \equiv \frac{1}{|\mathbf{r}_1|} \sum_{i=1}^{L} \langle \mathbf{r}_1 \cdot \mathbf{r}_i \rangle. \tag{2.17}$$

In Appendix B we follow the same lines of argument as Yamakawa[9] to arrive at the acquired expressions for the calculation of those length scales.

We look upon a homopolymer as a chain of L bonds with identical bond lengths b and bond angles θ between bond vectors $\mathbf{r}_i$ and $\mathbf{r}_{i+1}$. The rotational angles are described within a rotational isomeric state model, where the energy difference between the *trans* and the *gauche* state is denoted by Δu_{tg}. For sufficiently long polymer chains the end-to-end distance and the persistence length are then given by

$$\langle R^2 \rangle_\infty = L b^2 \frac{2\omega + 4}{3\omega}, \tag{2.18}$$

$$q_\infty = b \frac{5\omega + 4}{6\omega}, \tag{2.19}$$

where $\omega = \exp(-\Delta u_{tg}/k_B T)$. When calculating the two discussed length parameters, we will use the number of segments N instead of L, which implies that $N \approx N - 1$.

III. RESULTS AND DISCUSSION

The main goal of our analysis of semi-flexible polymers near a liquid–liquid interface is to relate adsorption behavior to the three relevant length scales in the system, ξ, q, and $\langle R^2 \rangle^{1/2}$. To make the discussion more transparent all variables are made dimensionless in the following way

$$\xi/b \to \xi, \quad z/b \to z, \quad q_\infty/b \to q_\infty, \quad \frac{\Delta u_{tg}}{k_B T} \to \Delta u_{tg}. \tag{3.1}$$

The stiffness of the polymer A_N is reflected in the persistence length q, in the RIS scheme determined by the energy difference Δu_{tg}. For large N this length scale is given by Eq. (2.19). It should be noted that the so determined persistence length may only be used as long as $q_\infty < N$.

The interfacial width ξ is mainly determined by the interaction between components C and D, which, in the SCF approach, is reflected in the Flory-Huggins parameter χ.

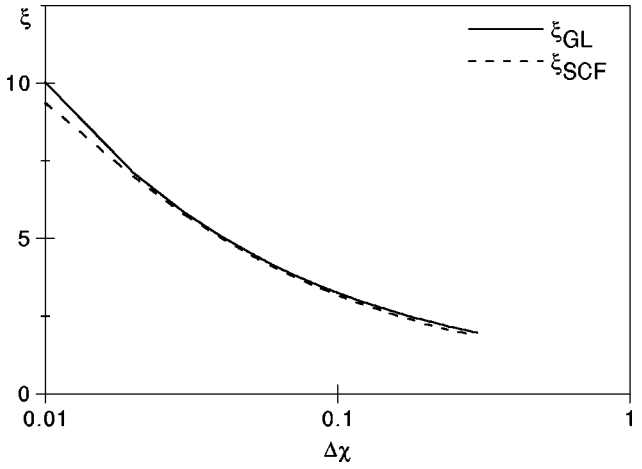

FIG. 1. Interfacial width as a function of $\chi - \chi_c$, calculated with the Ginzburg-Landau approximation [Eq. (2.6)] and with the SF SCF model ($m = 300$).

From the SCF calculations for a 2-component system, ξ is calculated from the slope of the reduced density profile at $z = 0$ as follows

$$2(\rho(m/2+1) - \rho_c)\xi = \rho(m) - \rho_c, \tag{3.2}$$

where ρ_c is the reduced density at the critical point. To show that ξ_{GL}, as given by Eq. (2.6), does not deviate much from that determined from SCF calculations, we plot both quantities in Fig. 1. The fact that $\xi_{SCF} < \xi_{GL}$, even near the critical point, is caused by two effects. The first is that the slope $d\rho/dz$ at $z = 0$ is underestimated due to the finite width of a lattice layer. The second is that for large ξ, i.e., close to the critical point, the number of lattice layers m should be increased to ensure that $\rho(m) = \rho^b$. Bearing these limitations in mind, the agreement between the two quantities is quite satisfactory. Hence, we can vary the value of χ to obtain the desired ξ.

A. Adsorbed amount

From the composition profiles, calculated with the SCF theory, we can determine the excess amount of polymer A_N, which we shall call the adsorbed amount

$$\theta_A^{exc} = -\rho_A^b m + \sum_{i=1}^{m} \rho_A(i). \tag{3.3}$$

Note that the term $\rho_A^b m$ can only be used in a symmetrical system, and should be replaced by two terms if the bulk densities are unequal in both phases. We will use this adsorbed amount to compare the behavior of our system for different values of the length parameters.

Figure 2 depicts the adsorption of A_{100} for given values of ξ as a function of the ratio q_∞/ξ. The most remarkable feature extracted from these curves is the minimum in θ_A^{exc}, which is located at q_∞ is of order (but higher than) ξ. The occurrence of this minimum can be understood in the following way. If q_∞/ξ is small, the polymer behaves (more or less) as a flexible coil, and adsorbs at the interface to reduce the unfavorable C–D contacts. An increase of the persistence length causes the polymer dimension to increase. This causes

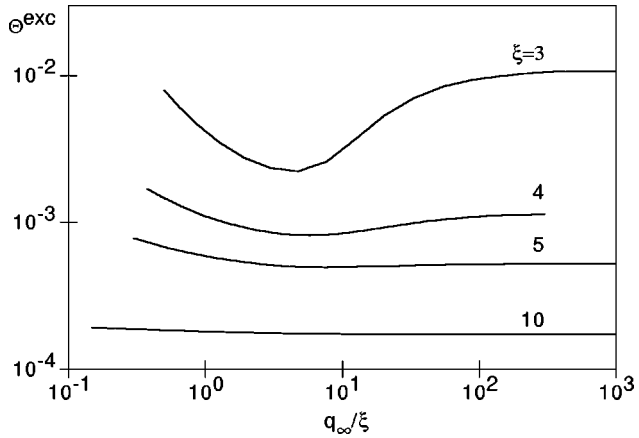

FIG. 2. Adsorbed amount as a function of the ratio between the persistence length and the interfacial width for different values of ξ at $N=100$.

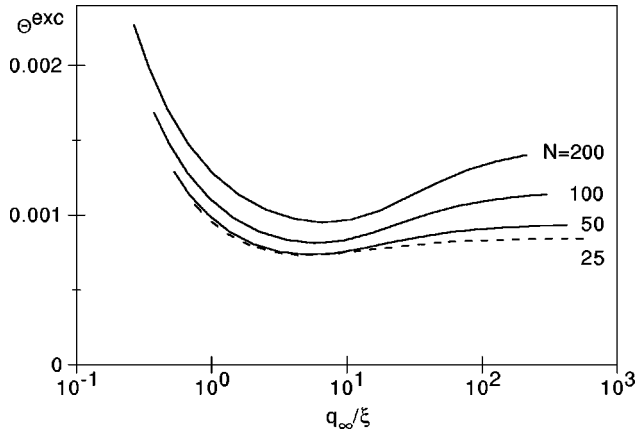

FIG. 4. Adsorbed amount for different chain lengths N with $N^{1/2}/\xi=5/2$, again as a function of q_∞/ξ.

the exclusion of other polymer chains from the interface, which leads to a decrease of the adsorbed amount. A further increase of q_∞ effectively changes the polymer chains into stiff objects in comparison to the interfacial width, for which the entropy loss upon adsorption becomes less, and they will align both to each other and to the interface. This alignment causes the adsorbed amount to increase. The levelling off of the curves at even higher q_∞ is due to the fact that there $q_\infty \gg N$, which means that the chains are effectively rods.

The fact that the shape of the curves in Fig. 2 changes with increasing interfacial width is caused by our choice of parameters for the calculation. Here, we neglected the effect of the third length scale, $\langle R^2\rangle^{1/2}$, on the adsorption behavior. Instead of changing ξ, while keeping N constant, one could vary N in such a way that $N^{1/2}/\xi$ remains constant. The factor $N^{1/2}$ stems from Eq. (B16), which states that $\langle R^2\rangle \propto N$. So, this way we effectively keep the ratio of the end-to-end distance to the interfacial width constant. One should bear in mind that this is only valid for long (semi-)flexible chains or, in other words, $1 \ll q_\infty \ll N$.

Figure 3 shows the adsorbed amount as a function of chain length N, where we kept q_∞/ξ and $N^{1/2}/\xi$ constant. Two important observations can be made. First, the adsorbed amount remains positive for all N. This can be easily understood by the fact that any third component in our system for which both C and D are good solvents, will decrease the number of unfavorable contacts between the monomeric solvents when adsorbed. In other words, there is an effective adsorption energy. Second (and more importantly), the additional adsorbed amount scales with $N^{1/2}$ (for large N), which indicates that N is indeed the only remaining relevant parameter for the shape of the adsorption curve if q_∞/ξ and $N^{1/2}/\xi$ are fixed.

Having made these observations, we expect that, when plotting Θ_A^{exc} as a function of q_∞/ξ for different values of N while keeping $N^{1/2}/\xi$ constant, these curves should have the same shape. That this is indeed the case is seen in Fig. 4, where $N^{1/2}/\xi=5/2$. This is even more clear when Θ_A^{exc} is related to its value at the minimum of the curve (or to any other point where $q_\infty \gtrsim 1$ and $q_\infty < N$). The latter procedure is equivalent to comparing the q_∞-dependent adsorbed amount from Fig. 4 to the N-dependent one plotted in Fig. 3. For large N it is possible to rescale the adsorption curves as $\Theta_A^{exc}/(\Theta_0^{exc}+\nu N^{1/2})$, where $\nu = d\Theta_A^{exc}/dN$ for large N, and Θ_0^{exc} is the extrapolation of the adsorbed amount $N \to 0$ from large N (see Fig. 3). Figure 5 shows that there is an almost perfect collapse of the curves on a ''mastercurve'' for the different chain lengths as long as $q_\infty/\xi < 20$. The deviation of the curves beyond this point is obvious, if one realizes that

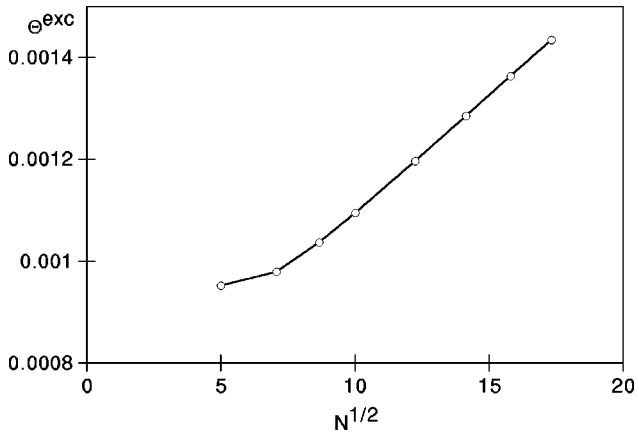

FIG. 3. Chain-length dependence of the adsorbed amount for $q_\infty/\xi=1$ and $N^{1/2}/\xi=5/2$.

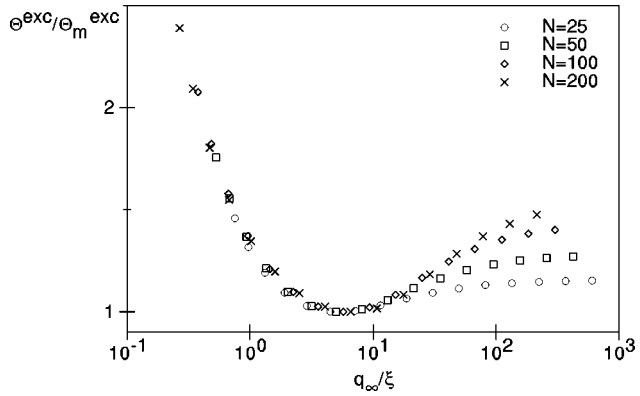

FIG. 5. Relative adsorbed amount related to Θ_{min} at the minimum of the curve. All data are taken from Fig. 4.

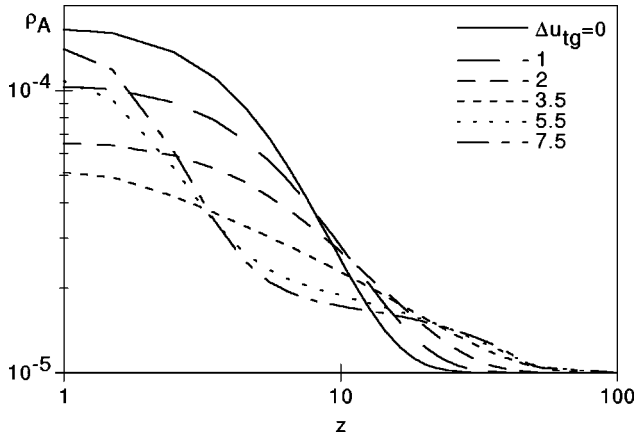

FIG. 6. Reduced density profiles of A_{100} for $\xi=4$ at different values of Δu_{tg}, corresponding to $q_\infty=1.5$, 2.6, 5.8, 23, 160, 1200.

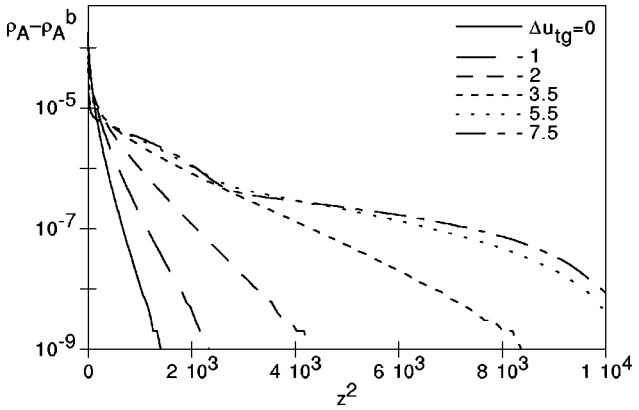

FIG. 7. Reduced density profiles of A_{100} compared to the bulk reduced density. Data as in Fig. 6.

the chain length is the limiting factor. The deviation occurs when $q_\infty \gtrsim N$, so the ''real'' shape of the adsorption curve can only be found for very large N. This observation can also be understood in terms of the fact that the adsorbed amount for rods will be proportional to N, which is not the case for the semi-flexible objects as was concluded from Fig. 3. In other words, we kept $N^{1/2}/\xi$ fixed instead of $\langle R^2\rangle^{1/2}$.

B. Density profiles

The observations for the adsorbed amounts of A_N can be further illustrated by taking a closer look at the composition profiles. Figure 6 gives the reduced density profiles of the systems corresponding to a few points on the curve in Fig. 4 for $N=100$. Due to the symmetry of the system, it is sufficient to show only the positive part of the z-axis. Clearly, the transition from a semi-flexible to rodlike conformation of the polymer chain is reflected in these profiles. One observes that by increasing the chain stiffness, the polymer initially penetrates more into the solution, whereas ρ_A decreases near the interface. However, when the chains become rodlike, the density at $z=0$ increases again, indicating alignment with the interface. The small fraction of rodlike chains that extent into the solution must do so over their full length. The decreases of the density at intermediate distance from the interface for rodlike chains also implies alignment.

To visualize the penetration of the polymer into the solution, $\rho_A-\rho_A^b$ is plotted in Fig. 7 as a function of z^2. Both flexible and semi-flexible objects show a more or less exponential decrease of the excess reduced density with the square of the distance from the interface. This indicates a Gaussian distribution of the polymer around the C–D phase boundary. Clearly, the reduced density profiles for the stiffer polymers ($\Delta u_{tg}=5.5$ and $\Delta u_{tg}=7.5$) differ only slightly from each other, which indicates that the conformation of the molecules must be similar. This is what we expected, because in both cases $q_\infty > N$, which means we are dealing with stiff polymers, where the one characterized by $\Delta u_{tg}=7.5$ (i.e., $q_\infty=1200$) can be regarded as a rod. The kink in the reduced density profile for these two stiff polymers at $z \approx 50$ originates from the fact that modeling rodlike molecules on a lattice introduces artifacts. In this case, the use of a RIS scheme on a tetrahedral lattice allows six orientations for a rod: one parallel to the interface, one perpendicular to it, and four making an angle $\Phi=(\pi-\theta)/2$, where θ is the tetrahedral bond angle. The kink presumably originates from the latter four possible orientations. This conjecture is confirmed by similar calculations (not shown) carried out on a cubic lattice and using second-order Markoffian statistics. In that case such a kink does not show up due to the absence of orientations other than perpendicular and parallel to the interface.

The impact of the observed phenomena on the ongoing discussion about the question which molecule is more surface active in a mixture of flexible and stiff polymers[1–3] should be clear. In the Henry regime, as studied here, the adsorption in a mixture of two types of polymer, differing in stiffness only, is an additive property. From Fig. 2 we conclude that decreasing the interfacial width will eventually favor the adsorption of the stiff polymer over a flexible one. However, Figs. 2–5 make clear that the chain-length dependence on this preferential adsorption behavior plays an important role. It is evident that only rodlike polymers of sufficient length at a given interfacial width will show higher adsorbed amounts than their flexible counterpart. So, one can imagine that in a system where several types of polymer (only differing in chain stiffness) are present, the precise associated length scales will be of major importance. This is the primary reason that the observations made in literature about preferential adsorption in such systems are sometimes contradicting.[1–3] We expect that preferential adsorption of sufficiently long rodlike polymer chains will occur at both sharp and smooth interfaces. Short rodlike polymers will only adsorb preferentially at sharp interfaces.

IV. CONCLUSIONS

We have shown that the adsorption of semi-flexible polymers onto a liquid–liquid interface is strongly influenced by the competition between the different length scales in the system. Increasing the stiffness of a polymer chain gives rise to a minimum in the adsorbed amount at a certain persistence length. This phenomenon originates from the transition of the polymer from flexible to rodlike, but also depends on the width of the interfacial region and the chain length. This

observation is also of importance for preferential adsorption problems, where one is interested in whether a stiff or a flexible polymer is more likely to adsorb. However, in this perspective one should also be aware of the fact that it is in practice difficult to change the stiffness of molecules without changing other interactions. Related to this drawback, it should be stressed that in several experimental systems enthalpic effects play a more important role than entropic ones.[10,11] In other words, when one tries to change the stiffness of a polymer, one possibly also changes its energetic interactions with its surroundings. If this is the case, this leads to a system differing substantively from the ones discussed in this paper. Therefore, experimental studies to verify the above results will be hard, but not impossible, to find.

We showed that if only one type of polymer is present, the adsorbed amount is very sensitive to different length parameters. This leads to the key conclusion that especially the interfacial width should be taken into account when studying adsorption of polymers with variable flexibility (or stiffness).

APPENDIX A: MEAN-FIELD ISING MODEL

To access the properties of a binary mixture we start from an Ising model. We choose the local composition variable $s_i=0,1$ for a site occupied by either C or D, respectively. A composition profile is determined by averaging over this variable, thus the local reduced density of D is given by

$$\rho_i=\langle s_i\rangle. \tag{A1}$$

If we only consider two-body interactions between the components, the exact Hamiltonian can be written as a function of the local composition variable s_i:

$$\mathcal{H}=\frac{1}{2}\sum_{ij}\ J_{ij}s_i(1-s_j), \tag{A2}$$

where J_{ij} is the net interaction between the C and D component. Due to the coupling between the sites, the partition function of this Hamiltonian is difficult to evaluate. As a model system we choose one which only depends on single-site variables. The model Hamiltonian can then be written in terms of the model parameters β_i

$$\mathcal{H}_0=k_{\mathrm{B}}T\sum_i\ \beta_i s_i\,. \tag{A3}$$

The least upper bound to the exact free energy $\mathcal{F}$ is found by minimizing F from Eq. (2.4) with respect to the parameters β_i. This upper bound is also the best estimate in the variational approach. The integration over phase space, $\int d\Lambda$, is now given by $\Pi_i\Sigma_{\{s_i\}}$, where $\{s_i\}$ denotes the set of possible values for s_i. Because of boundary conditions, the locally average compositions and, hence, β_i may vary in space. We are interested in a binary system beyond its critical point, where an interface exists, so that such a spatial variation does indeed occur.

For the free energy and for the partition function of the model system we may write

$$F_0=-k_{\mathrm{B}}T\ \ln\ Z_0,\quad Z_0=\prod_i\ \sum_{\{s_i\}}\ e^{-\beta_i s_i}=\prod_i\ \frac{1}{1-\rho_i}, \tag{A4}$$

with $\rho_i=(1+e^{\beta_i})^{-1}$. Averaging s_i with respect to P_0 results in

$$\langle s_i\rangle_0=\frac{\Sigma_{\{s_i\}}s_i e^{-\beta_i s_i}}{\Sigma\{s_i\}e^{-\beta_i s_i}}=\rho_i\,. \tag{A5}$$

The variable ρ will be used to describe the reduced density profile of our system. It is easily shown that

$$\langle\mathcal{H}-\mathcal{H}_0\rangle=\frac{1}{2}\sum_{ij}\ J_{ij}\rho_i(1-\rho_j)-\sum_i\ \beta_i\rho_i\,. \tag{A6}$$

Substituting Eqs. (A4) and (A6) in Eq. (2.4) gives us the upper bound of the free energy of the system

$$F=k_{\mathrm{B}}T\sum_i\ ((1-\rho_i)\ln(1-\rho_i)+\rho_i\ \ln\ \rho_i)+\frac{1}{2}\sum_{ij}\ J_{ij}\rho_i(1-\rho_i). \tag{A7}$$

This equation is the generalization of the free energy of a homogeneous system in the random mixing approximation, i.e., the composition variable can vary in space. The composition variables ρ_i can now be regarded as the variational parameters to minimize F with fixed overall composition. In fact one minimizes $G=F-\Sigma_i\mu\rho_i$. In our system an interface is present, which implies that ρ_i varies in space. Minimization is most effectively done in the continuum limit since this will lead to differential equations instead of finite difference equations.

Taking the continuum limit of Eq. (A7) is done by noting that

$$J_{ij}\rho_i(1-\rho_j)=\frac{1}{2}J_{ij}((\rho_i-\rho_j)^2-\rho_i^2-\rho_j^2+2\rho_i). \tag{A8}$$

We will change to a notation for a free energy per unit volume, which allows us to convert $\rho_i-\rho_j$ to a gradient. We only take into account nearest-neighbor interactions, i.e., J_{ij} is only nonzero if site i and j are adjacent. Doing this, we may write

$$(\rho_i-\rho_j)\mapsto b\nabla\rho, \tag{A9}$$

where b is the nearest-neighbor distance. Obviously, $\rho_i\mapsto\rho(\mathbf{r})$, which gives the continuum version of Eq. (A7)

$$F=\int d\mathbf{r}\left(f_0(\rho(\mathbf{r}))+\frac{1}{2}B|\nabla\rho(\mathbf{r})|^2\right), \tag{A10}$$

where $f_0(\rho)$ is defined in Eq. (A11) and $B=2\lambda_1\chi k_{\mathrm{B}}T/b$. We choose to use the Flory-Huggins interaction parameter, here defined as $\chi=(1/2k_{\mathrm{B}}T)\,\Sigma_j J_{ij},\forall i$. The parameter λ_1 originates from the type of underlying lattice, and also appears in the self-consistent field approach. It accounts for the relative number of nearest neighbors of a segment in the direction of the reduced density gradient. For a tetrahedral lattice $\lambda_1=1/4$. Equation (A10) is also known as the square gradient approach, which was already used by Van der

Waals to describe the liquid–vapor interface.[12] However, it were Cahn and Hilliard[13] who made this method ''popular.'' The local part of the free energy density is given by

$$f_0(\rho)=\frac{k_BT}{b^3}(\rho\ \ln\ \rho+(1-\rho)\ln(1-\rho)+\chi\rho(1-\rho)). \tag{A11}$$

We now have the free energy as a functional of the local, average composition. We can find the spatial variation in this by minimizing F with respect to $\rho(\mathbf{r})$ with the appropriate boundary conditions. Unfortunately, using Eq. (A11) there is no analytical solution. However, near the critical point ($\rho=1/2$), one can expand f_0 about $\Psi=\rho-1/2$, which gives

$$f_0\approx\frac{k_BT}{b^3}\left(2\Psi^2+\frac{4\Psi^4}{3}-\ln 2+\chi\left(\frac{1}{4}-\Psi^2\right)\right). \tag{A12}$$

This approach is known as the Ginzburg-Landau expansion of the free energy. Using this approximation, we can write for the Helmholtz free energy

$$F=\int d\mathbf{r}\left(-\frac{\epsilon}{2}\Psi^2+\frac{c}{4}\Psi^4+\frac{B}{2}|\nabla\Psi|^2\right), \tag{A13}$$

where constant terms in the integral are dropped, because they are irrelevant in finding the minimum of F. Furthermore, we apply the constraint that the total composition remains unchanged [i.e., $\int d\mathbf{r}\rho(\mathbf{r})$ is fixed]. The coefficients in Eq. (A13) are given by $\epsilon=(2\chi-4)k_BT/b^3$ and $c=16k_BT/(3b^3)$.

We look for the minimization of F for a system with an interface, such that

$$\Psi\rightarrow\pm\Psi_0 \quad \text{if} \quad z\rightarrow\pm\infty. \tag{A14}$$

To this end, we apply calculus of variations[14] that minimizes the functional

$$F=\int d\mathbf{r}f(\Psi,\nabla\Psi) \tag{A15}$$

with respect to all possible variations of $\Psi(\mathbf{r})$. The function f which minimizes F is given in Einstein notation by

$$\frac{\partial F}{\partial\Psi(\mathbf{r})}=\frac{\partial f}{\partial\Psi}-\frac{\partial}{\partial r_i}\frac{\partial f}{\partial\Psi_{r_i}}=0, \tag{A16}$$

where $\Psi_{r_i}=\partial\Psi/\partial r_i$. This results in

$$-\epsilon\Psi+c\Psi^3-B\nabla^2\Psi=0 \tag{A17}$$

with the appropriate boundary conditions. Assuming the system to have its equilibrium bulk values far away from the interface, it is easily seen that these composition values are given by

$$\Psi\rightarrow\pm\Psi_0=\pm\sqrt{\frac{\epsilon}{c}}. \tag{A18}$$

In the present system, a one-dimensional concentration variation $\Psi(z)$ is likely, and $d\Psi/dz=0$ at $z\rightarrow\pm\infty$. The solution of Eq. (A17) is then given by

$$\Psi(z)=\sqrt{\frac{\epsilon}{c}}\tanh\frac{z}{\xi}, \tag{A19}$$

where the interfacial width, or bulk correlation length, is given by

$$\xi=\sqrt{\frac{2B}{\epsilon}}=b\sqrt{\frac{2\lambda_1\chi}{\chi-2}}. \tag{A20}$$

APPENDIX B: CHAIN DIMENSIONS WITHIN THE ROTATIONAL ISOMERIC STATE MODEL

We depict a homopolymer as a chain of L bonds with identical bond lengths b and bond angles θ between bond vectors $\mathbf{r}_i$ and $\mathbf{r}_{i+1}$. We take the rotation angles ϕ_i as internal coordinates, where we denote $\{\phi_L\}=\phi_1,\phi_2,\ldots,\phi_L$. The configurational partition function is written as

$$Z=\int d\{\phi_L\}\exp\left(-\frac{U(\{\phi_L\})}{k_BT}\right), \tag{B1}$$

where U is the energy, strictly the potential of mean force, of internal rotation. The crux of the problem is to express $\mathbf{r}_i\cdot\mathbf{r}_j$ in terms of $\{\phi_L\}$. The matrix formalism, first suggested by Eyring,[15,16] can be used for this purpose.

Every bond vector is linked to a Cartesian coordinate system, where the positive direction of the x_j axis coincides with $\mathbf{r}_j$. The positive direction of the y_j axis makes an acute angle with $\mathbf{r}_{j-1}$ and is in the same plane as $\mathbf{r}_j$ and $\mathbf{r}_{j-1}$. The z_j axis is chosen such that it forms a right-handed coordinate system with the x_j and y_j axes. The rotation angle ϕ_j about $\mathbf{r}_{j-1}$ is defined by the angle between the two planes containing $\mathbf{r}_{j-2}$ and $\mathbf{r}_{j-1}$, and $\mathbf{r}_{j-1}$ and $\mathbf{r}_j$, respectively. When $\mathbf{r}_{j-2}$ and $\mathbf{r}_j$ are in the *trans* position with respect to each other, $\phi_j=0$, and it takes positive values when $\mathbf{r}_j$ lies in the positive range of the z_{j-1} axis. To transform the jth coordinate system into the $(j-1)$th one, one uses the orthogonal matrix

$$\mathbf{A}_j=\begin{pmatrix}-\cos\theta & \sin\theta & 0\\ \sin\theta\cos\phi_j & \cos\theta\cos\phi_j & \sin\phi_j\\ \sin\theta\sin\phi_j & \cos\theta\sin\phi_j & -\cos\phi_j\end{pmatrix}. \tag{B2}$$

The bond vector $\mathbf{r}_j$ is represented in the $(j-1)$th coordinate system by $\mathbf{A}_j\mathbf{b}$, where $\mathbf{b}$ denotes the column vector $(b\ 0\ 0)$ representing $\mathbf{r}_j$ in its own coordinate system. This procedure can be repeated to arrive at a representation in the ith coordinate system. The average of the scalar product of two bond vectors can be written as

$$\langle\mathbf{r}_i\cdot\mathbf{r}_j\rangle=\mathbf{b}^T\left\langle\prod_{k=1+i}^{j}\mathbf{A}_k\right\rangle\mathbf{b}. \tag{B3}$$

With the aid of Eq. (B1) the average on the right-hand side is given by

$$\left\langle\prod_{k=1+i}^{j}\mathbf{A}_k\right\rangle=Z^{-1}\int d\{\phi_L\}\left(\exp\left(-\frac{U(\{\phi_L\})}{k_BT}\right)\prod_{k=1+i}^{j}\mathbf{A}_k\right). \tag{B4}$$

The problem now reduces to finding a suitable form for the energy U. It should enables us to introduce chain stiffness and should also be useful in the self-consistent field calculations.

A realistic model includes first and second neighbor interactions. This is achieved by writing the energy as

$$U(\{\phi_L\})=\sum_{i=1}^{L} u_{1i}(\phi_i)+\sum_{i=1}^{L} u_{2i}(\phi_i,\phi_{i+1}). \tag{B5}$$

It is convenient to discretize the energy in order to simplify calculations. A suitable approximation for this purpose is the rotational-isomeric state model, where ϕ_i can only take a discrete number of fixed values, which we will denote as $\phi_i^{(k)}$ $(k=1,2,\ldots,\kappa)$. These rotational angles correspond to the local minima of U. Keeping in mind the lattice theory which we use, a 3-state model is obvious. We will consider three available states, T (*trans*, $\phi^{(1)}=0$), G (*gauche*, $\phi^{(2)}=2\pi/3$), and G' (another *gauche*, $\phi^{(3)}=-2\pi/3$). With this approximation we can rewrite the partition function of Eq. (B1) as

$$Z=\sum_{\{\phi_L\}}\prod_{i=1}^{L} p(\phi_i,\phi_{i+1}), \tag{B6}$$

where

$$p(\phi_i,\phi_{i+1})=\exp\left(-\frac{u_1(\phi_i)+u_2(\phi_i,\phi_{i+1})}{k_BT}\right). \tag{B7}$$

This approach requires a value for ϕ_{L+1}, which we will assume to be ϕ_1. To tackle the present problem elegantly we introduce a 3×3 matrix $\mathbf{p}$ which is represented by

$$p_{kl}=p(\phi_i^{(k)},\phi_{i+1}^{(l)}), \tag{B8}$$

where p_{kl} is independent of i. Diagonalization of $\mathbf{p}$ is done by $\mathbf{\Lambda}(\lambda_i)=\mathbf{Q}^{-1}\mathbf{pQ}$, where λ_i are the eigenvalues of $\mathbf{p}$. Equation (B6) simplifies to

$$\begin{aligned} Z&=\text{trace }\mathbf{p}^L=\sum_{i=1}^{3}\lambda_i^L \\ &\approx\lambda^L \quad (\text{for large } L), \end{aligned} \tag{B9}$$

where λ is the largest eigenvalue. Along the same lines we can express the average of a product of functions $g_i(\phi_i)$ as follows

$$\begin{aligned} \left\langle\prod_{k=i+1}^{j} g_k(\phi_k)\right\rangle &= Z^{-1}\sum_{\{\phi_L\}}\left(\prod_{k=i+1}^{j} g_k(\phi_k)\right) \\ &\quad\times\left(\prod_{i=1}^{L} p(\phi_i,\phi_{i+1})\right) \\ &= Z^{-1}\ \text{trace }\mathbf{g}_{i+1}\left(\prod_{k=i+2}^{j}\mathbf{pg}_k\right)\mathbf{p}^{L-(j-i-1)} \\ &\approx \mathbf{yg}_{i+1}\left(\prod_{k=i+2}^{j}\lambda^{-1}\mathbf{pg}_k\right)\mathbf{x} \quad (\text{for large } L), \end{aligned} \tag{B10}$$

where $\mathbf{g}_i$ is the diagonal matrix with elements $g_i(\phi^{(k)})$, and $\mathbf{x}$ and $\mathbf{y}$ are normalized right-hand and left-hand eigenvectors of $\mathbf{p}$, respectively, i.e.,

$$\mathbf{px}=\lambda\mathbf{x}, \quad \mathbf{yp}=\lambda\mathbf{y}, \quad \mathbf{yx}=1. \tag{B11}$$

We are interested in the element A_{rs} of the product of transformation matrices $\mathbf{A}_k$, which is of the form $g_{i+1}\ldots g_j$. Using Eq. (B10) we obtain

$$\langle A_{rs}\rangle=\mathbf{y}\sum_t\cdots\sum_v \mathbf{a}_{rt}(\lambda^{-1}\mathbf{pa}_{tu})\cdots(\lambda^{-1}\mathbf{pa}_{vs})\mathbf{x}, \tag{B12}$$

where $\mathbf{a}_{ij}$ represents the diagonal matrix with diagonal elements $a_{ij}(\phi^{(k)})$ with $a_{ij}(\phi)$ being the elements of $\mathbf{A}$. In short-hand notation Eq. (B12) reads

$$\left\langle\prod_{k=i+1}^{j}\mathbf{A}_k\right\rangle=\mathbf{YTS}^{j-i-1}\mathbf{X} \tag{B13}$$

with

$$\mathbf{S}=\lambda^{-1}\mathbf{PT}, \tag{B14}$$

where the ''elements'' $\mathbf{a}_{ij}$ constitute the matrix $\mathbf{T}$, resulting in a 9×9 matrix. The matrices $\mathbf{P}$, $\mathbf{X}$, and $\mathbf{Y}$ are defined as the direct products

$$\mathbf{P}=\mathbf{p}\times\mathbf{I}_3, \quad \mathbf{X}=\mathbf{x}\times\mathbf{I}_3, \quad \mathbf{Y}=\mathbf{y}\times\mathbf{I}_3, \tag{B15}$$

where $\mathbf{I}_s$ denotes a $s\times s$ unit matrix. Combination of Eqs. (B13), (B3), and (2.16) leads to the following expression for the end-to-end distance

$$\langle R^2\rangle=Lb^2(1+2\mathbf{e}^T\mathbf{YT}(\mathbf{I}_9-\mathbf{S})^{-1}\mathbf{Xe}) \quad (\text{for large } L) \tag{B16}$$

with $\mathbf{e}=(1\ 0\ 0)$ the unit bond vector. This expression was first derived by Lifson[17] and Nagai,[18] independently. Along the same lines, using Eq. (2.17), the expression for the persistence length reads

$$q=b(1+\mathbf{e}^T\mathbf{YT}(\mathbf{I}_9-\mathbf{S})^{-1}\mathbf{Xe}) \quad (\text{for large } L). \tag{B17}$$

The last step before we can calculate q and $\langle R^2\rangle$ is to write $\mathbf{p}$ from Eq. (B8) in explicit form and take a value for the bond angle θ. The latter is conveniently chosen as the tetrahedral angle, for which $\cos\theta=-1/3$. We choose the potential $u_1(\phi^{(1)})$ in the *trans* state as the zero of energy, and assume the following statistical weights for the different conformations: 1 (T), ω (G,G'), and 1 $(TT,TG,TG',GT,G'T,GG,G'G',GG',G'G)$. With these definitions the matrix can be written as

$$\mathbf{p}=\begin{pmatrix} 1 & 1 & 1 \\ \omega & \omega & \omega \\ \omega & \omega & \omega \end{pmatrix}, \tag{B18}$$

with $\omega=\exp(-\Delta u_{tg}/k_BT)$, where the energy difference Δu_{tg} between the *trans* and the *gauche* state is the same as the one introduced in Sec. II C. It should be noted that these assumptions neglect the so-called pentane effect,[19,20] which is in accordance with the present implementation of the RIS model in the SF SCF theory. Substitution of this explicit form of $\mathbf{p}$ into Eqs. (B16) and (B17) leads to surprisingly simple equations for the end-to-end distance and the persistence length of relatively long polymers:

$$\langle R^2\rangle_\infty=Lb^2\frac{2\omega+4}{3\omega}, \tag{B19}$$

$$q_\infty=b\frac{5\omega+4}{6\omega}. \tag{B20}$$

[1] A. Yethiraj, S. Kumar, A. Hariharan, and K. S. Schweizer, J. Chem. Phys. **100**, 4691 (1994).
[2] S. K. Kumar, A. Yethiraj, K. S. Schweizer, and F. A. M. Leermakers, J. Chem. Phys. **103**, 10 332 (1995).
[3] D. T. Wu, G. H. Fredrickson, and J. P. Carton, J. Chem. Phys. **104**, 6387 (1996).
[4] J. P. Hansen and I. R. McDonald, *Theory of Simple Liquids* (Academic, New York, 1985), p. 152.
[5] S. A. Safran, *Statistical Thermodynamics of Surfaces, Interfaces, and Membranes* (Addison-Wesley, Reading, 1994).
[6] J. M. H. M. Scheutjens and G. J. Fleer, J. Phys. Chem. **83**, 1619 (1979).
[7] J. M. H. M. Scheutjens and G. J. Fleer, J. Phys. Chem. **84**, 178 (1980).
[8] F. A. M. Leermakers and J. M. H. M. Scheutjens, J. Chem. Phys. **89**, 3264 (1988).
[9] H. Yamakawa, *Modern Theory of Polymer Solutions* (Harper & Row, New York, 1971), Chap. 2.
[10] R. A. L. Jones, E. J. Kramer, M. Rafailovich, J. Solkolov, and S. A. Schwarz, Phys. Rev. Lett. **62**, 280 (1989).
[11] A. Hariharan, S. K. Kumar, and T. P. Russell, J. Chem. Phys. **98**, 4163 (1993).
[12] J. D. van der Waals, Verhand. Kon. Akad. v. Wetensch. (1e Sectie) **1**, 1 (1983).
[13] J. W. Cahn and J. E. Hilliard, J. Chem. Phys. **28**, 258 (1958).
[14] G. Arfken, *Mathematical Methods for Physicists* (Academic, New York, 1985).
[15] H. Eyring, Phys. Rev. **39**, 746 (1932).
[16] F. T. Wall, J. Chem. Phys. **11**, 67 (1943).
[17] S. Lifson, J. Chem. Phys. **30**, 964 (1959).
[18] K. Nagai, J. Chem. Phys. **31**, 1169 (1959).
[19] K. S. Pitzer, J. Chem. Phys. **8**, 711 (1940).
[20] W. J. Taylor, J. Chem. Phys. **16**, 257 (1948).